The Effect of Carbonated Brine on Well Cement Used in Geologic Formations.

A. Duguid[1], M. Radonjic[2], and G. W. Scherer[3]
[1]*Schlumberger Carbon Services, Pittsburgh, Pennsylvania, USA;* [2]*BP, Houston, Texas, USA;* [3]*Princeton University, Princeton, New Jersey, USA*

1 Introduction

Carbon sequestration in abandoned petroleum fields may be a short-term solution to reducing anthropogenic emissions of CO_2. If sequestration is adopted on a large scale, it will be important to understand how CO_2 may leak out of sequestration formations via abandoned wells. Within an abandoned petroleum well there are multiple pathways that CO_2 may use to escape to the atmosphere. These include leakage through the cement that makes up the primary and/or plug cement in the well, leakage through the interface between the primary cement and the geologic formation, and leakage through the interface between the well cement and the well casing. As the plume of carbonic acid created by sequestration reaches an abandoned well, the first potential pathway with which it comes in contact is the interface between the geologic formation and the primary well cement. In order to better understand what takes place when carbonic acid reaches the cement-rock interface, a series of batch experiments was conducted. This paper describes experiments that were conducted on composite samples that were made from Class H well cement and Salem limestone or Berea sandstone.

2 Materials and Methods

The samples used in the experiments were made from Class H well cement and Berea sandstone or Salem limestone. The samples were constructed by drilling a 25-mm hole along the long axis (but off center) in a 55-mm-diameter cylinder of rock and by filling the hole with neat cement paste (Figure 1). The cement paste was made according to API 10B [1] from Class H well cement (LaFarge Class H HSR) with a W/C = 0.38. Well cement with this W/C was also used by Bruckdorfer [2] and Onan [3] in their cement carbonation experiments. After curing for 7 months, the composite cylinders were sliced into samples about 8 mm tall. To ensure that fluid could only reach the cement radially, the faces of the samples were sealed with PTFE gasket material that was clamped on using 316

Contact E-mail: aduguid@slb.com

stainless-steel plates. The experiments were conducted at room temperature and 50°C and at ambient pressure over the course of a year. Samples were removed from reactor vessels at 0, 1, 2, 3, 6, and 12 months. The sandstone-cement samples were reacted using silicon-saturated carbonated brine (0.5*M* NaCl solution) at pH 3, 4, and 5. The limestone-cement samples were reacted in calcium-saturated carbonated brine at pH 5, 6, and 7. These are likely pHs for their respective formations at a 1-km depth based on calculations with EQ 3/6 version 8 [4]. The fluid in the reactor vessels was never replaced, but the pH was adjusted back to the original pH using HCl or NaOH if it varied by more than 0.2 pH units. The volume ratio of brine to sample was large enough, 25, to ensure quasi-constant boundary conditions.

The pH and composition data for the fluid in the batch reactors were collected throughout the experiment using a Thermo-Orion 230A pH probe and Perkin-Elmer ICP-OES. The cement-rock samples were used to collect permeability data and measure the depth of the reaction zone in the cement. The permeability data were collected using a GCTS triaxial cell to measure permeabilities on composite cement-stone and stone samples that were reacted at pH 3 and 5 for the sandstone-cement/sandstone samples and pH 5 and 7 for the limestone-cement/limestone samples. The depth of the visible reaction was measured for all the samples using a Nikon optical microscope. The measurements of the visible reaction depth were collected around the perimeter of the sample every 45 degrees starting at the thin side (3 mm thick stone), 0 degrees, and ending at the thick side (27 mm thick stone), 180 degrees (Figure 1). X-ray maps of the pH 3 sandstone-cement were also made on the 6-month sample using a Cameca 200 electron microprobe operated at 20 KV.

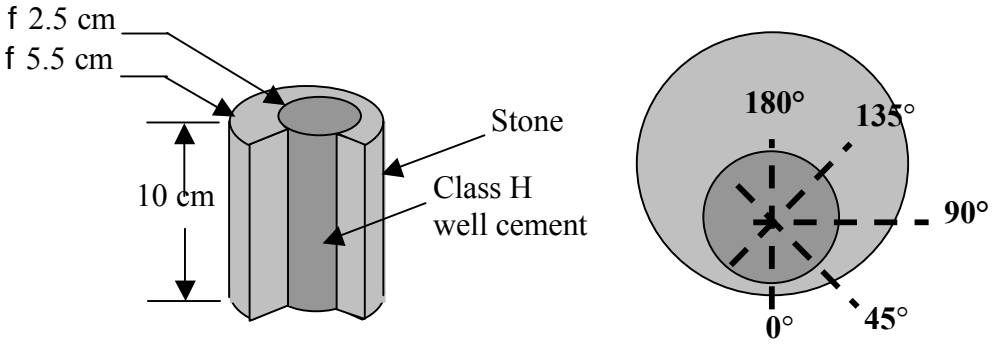

Figure 1 Sectioned schematic of a stone-cement sample prior to slicing (left). Measurement positions for the depth of visible reaction measurements (right).

3 Results

A visible reaction zone was apparent within the first month in all the sandstone-cement samples. In each set of room temperature sandstone-cement samples, the color of the reacted zone changed over the course of the experiment. At the 0-degree position after 1 month, it was a cream color. By the second month the zone had changed to a light orange. And by the end of the experiment the reacted zone was a bright orange at the interface, becoming lighter in color toward the center of the cement. Photos of the 0-degree sample position for the pH 3 sandstone-cement experiment are shown in Figure 2. The cement on the 50°C sandstone-cement samples showed a similar reaction, but the cement in these samples invaded the stone (about 2 mm), and so the reaction is in the pores of the stone and not in the bulk cement (Figure 3). The limestone-cement samples showed no visible signs of attack for the duration of the experiment.

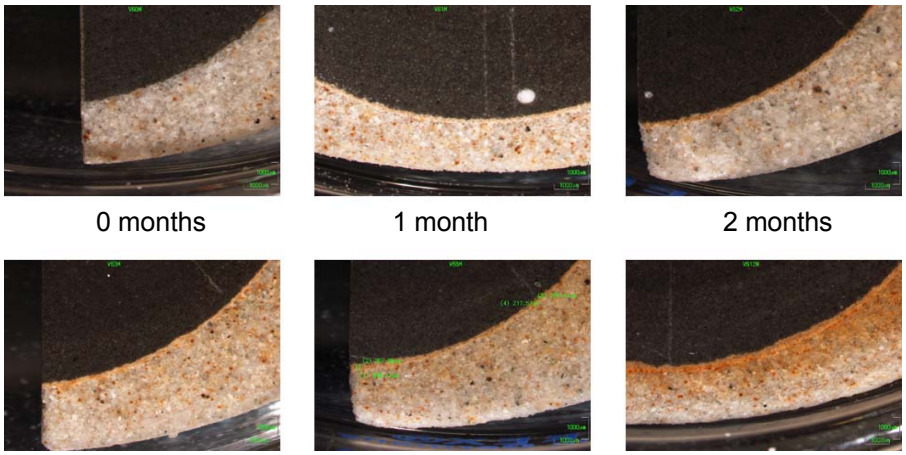

Figure 2 Photos showing the 0-degree position on room temperature sandstone-cement samples reacted at pH 3 over 12 months.

Measurements of the depth of the visible reaction zone showed that the depth of penetration at the interface of the sandstone-cement samples had a square root of time dependence over the first 6 months. Plots of the reaction depth data versus the Boltzmann variable ($t^{1/2}/r$, where t is time and r is the shortest distance to the perimeter of the sample) show a linear

shape over the first 6 months (Figure 4). After 6 months, the depth of penetration slowed, with very little change between 6 and 12 months.

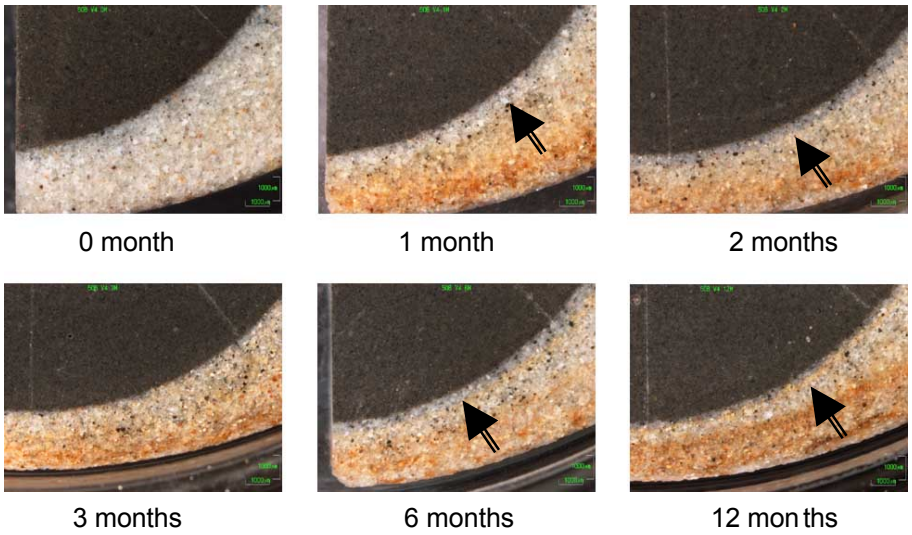

Figure 3 Photos showing the 0-degree position on 50°C sandstone-cement samples reacted at pH 3 over 12 months. Note: the black arrows identify the edge of the reaction zone.

The permeability of the room temperature sandstone-cement samples increases by approximately an order of magnitude over the course of the experiments, from near 2 x 10^{-14} m^2 to 3 x 10^{-13} m^2. The pH 3 set of samples exhibited the fastest rise in permeability, with almost all of the increase over the first month. The increase in permeability for the pH 5 sandstone-cement samples occurred over the first 3 months. After the increase, both sets of samples remained in the 10^{-13} m^2 range for the rest of the experiment. The permeability of the sandstone alone was generally in the 10^{-14} m^2 range for both experiments during the experiment. The limestone-cement samples did not show degradation at the interface and also did not show a rise in permeability over the 12 months. The permeability of the 50°C sandstone-cement samples increased from 4 x 10^{-14} m^2 to 4 x 10-13 m^2 during the experiment. The permeability of the 50°C sandstone increased from 3 x 10^{-14} m^2 to 3 x 10^{-13} m^2. The 50°C limestone-cement samples did not show degradation at the interface and also did not show a rise in permeability over the 12 months. It is important to note that each of the limestone-cement samples cracked near the 0-degree position while curing, so the permeability measurements are higher than those of the stone and the values are erratic. Plots of all of the permeability data versus time are shown in Figure 5.

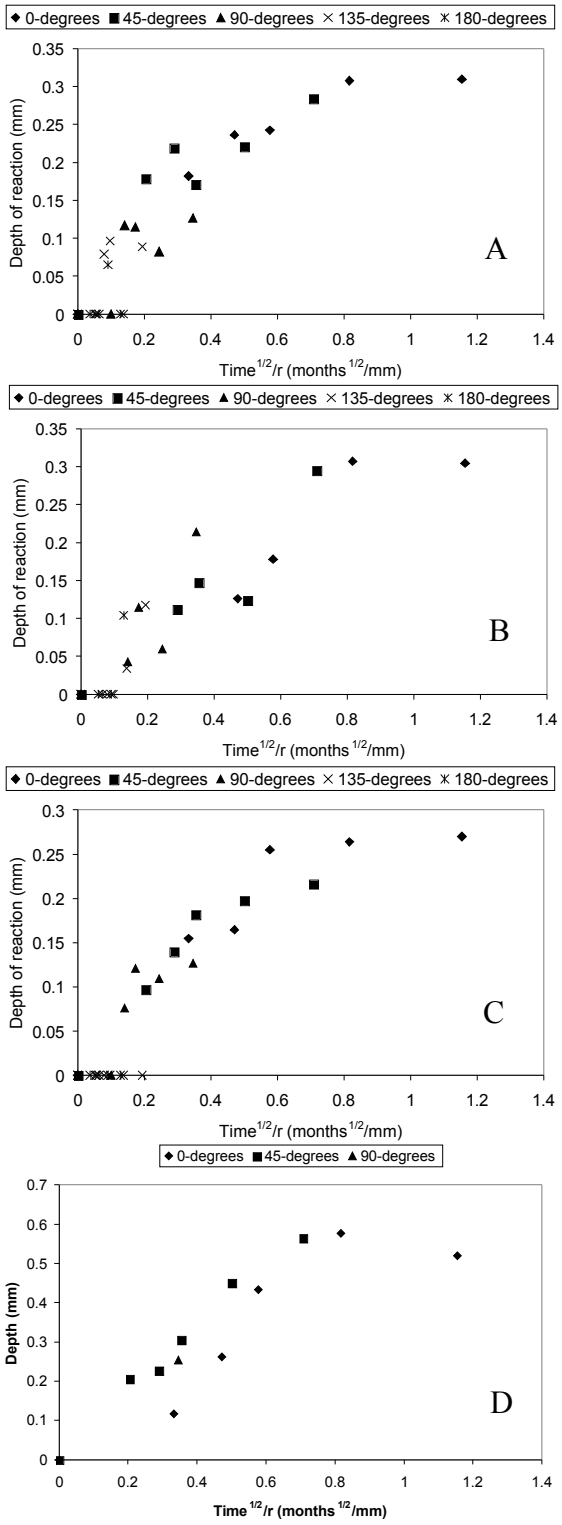
0-degrees
45-degrees
90-degrees
135-degrees
180-degrees
Depth of reaction (mm)
Time1/2/r (months1/2/mm)
A
B
C
D
Depth (mm)
Time 1/2/r (months 1/2/mm)

Figure 4 Plots of visible reaction depth versus the Boltzmann variable for sandstone-cement samples reacted at room temperature pH 3 (A), pH 4 (B), and pH 5 (C) and at 50°C pH 3 (D).

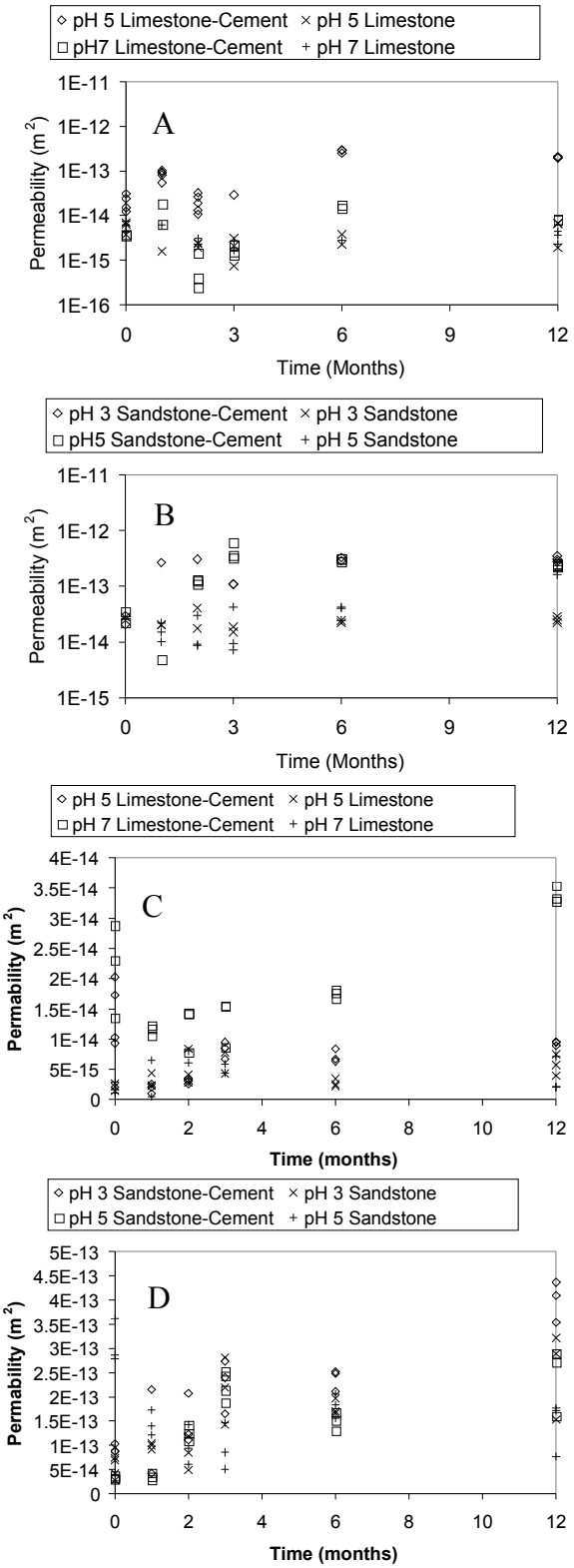

Figure 5 Permeability of room temperature samples (A) and (B) and 50°C samples (C) and (D).

ICP-EOS measurements of calcium, iron, magnesium, and silicon in the reactor fluids in the room temperature sandstone -cement experiments over the course of the experiment were plotted against the square root of time (Figure 6). The data show a linear trend over the first 10 $days^{1/2}$ (~3 months), after which the slope starts to become less steep and the spread in the data becomes greater. The data at pH 3 room temperature sandstone-cement data show that calcium and silicon concentrations increase throughout the experiment and iron and magnesium concentrations level off after 15 $days^{1/2}$ (~7.5 months). The slopes for the pH 3 data are 17.20 $mg/L/day^{1/2}$ (R^2 = 0.94) for calcium, 7.55 $mg/L/day^{1/2}$ (R^2 = 0.91) for iron, 3.20 $mg/L/day^{1/2}$ (R^2 = 0.99) for magnesium, and 0.66 $mg/L/day^{1/2}$ (R^2 = 0.98) for silicon.

Concentrations of all four constituents increase throughout the pH 4 sandstone-cement experiment. The slopes for the pH 4 room temperature sandstone-cement data are 12.20 $mg/L/day^{1/2}$ (R^2 = 0.95) for calcium, 2.57 $mg/L/day^{1/2}$ (R^2 = 0.88) for iron, 1.95 $mg/L/day^{1/2}$ (R^2 = 0.94) for magnesium, and 0.56 $mg/L/day^{1/2}$ (R^2 = 0.96) for silicon. The pH 5 room temperature sandstone-cement data show that calcium and magnesium increase over the course of the experiment, silicon levels off after about 13 $days^{1/2}$ (~6 months), and iron increases between 0 and 10 $days^{1/2}$ (0 and ~3 months) and then drops off to 0 mg/L between 10 and 15 $days^{1/2}$ (~3 and ~7.5 months). The slopes for the pH 5 room temperature sandstone-cement data are 11.72 $mg/L/day^{1/2}$ (R^2 = 0.98) for calcium, 1.08 $mg/L/day^{1/2}$ (R^2 = 0.72) for iron, 2.06 $mg/L/day^{1/2}$ (R^2 = 0.96) for magnesium, and 0.67 $mg/L/day^{1/2}$ (R^2 = 0.97) for silicon.

The ICP-EOS data for the room temperature limestone-cement experiments showed very little change in concentration for iron, magnesium, and silicon over the course of the experiment. The calcium concentrations for the limestone-cement experiments were too high to measure at pH 5 and 6 and were steady throughout the experiment for pH 7. Iron, magnesium, and silicon concentrations were steady throughout all of the 50°C limestone-cement experiments.

The pH 3 ICP-OES data for the 50°C sandstone-cement experiment show a linear trend for the first 3 months (10 $days^{1/2}$) when plotted against the square root of time. The slope for the pH 3 calcium data is 11.10

mg/L/day$^{1/2}$ (R^2 = 0.89), the slope value for iron is 5.58 mg/L/day$^{1/2}$ (R^2 = 0.86), the slope value for magnesium is 4.10 mg/L/day$^{1/2}$ (R^2 = 0.93), and the slope value for silicon is 1.02 mg/L/day$^{1/2}$ (R^2 = 0.64). At around 10 days$^{1/2}$ (~3 months) all of the curves seem to show a break, and then the data become too noisy to fit.

The data for the pH 4 50°C sandstone-cement experiments also show the first three months of the experiment to be linear. Using linear fits of the data for the first 3 months of the experiment, the slope for the calcium plot is 13.28 mg/L/day$^{1/2}$ (R^2 = 0.78), the slope value for magnesium is 3.34 mg/L/day$^{1/2}$ (R^2 = 0.55), and the slope value for silicon was 0.68 mg/L/day$^{1/2}$ (R^2 = 0.30). The data for the pH 5 experiment again show that the first three months of the experiment appear to be linear. Linear fits of these data give slopes of 10.79 mg/L/day$^{1/2}$ (R^2 = 0.89) for calcium, 3.50 mg/L/day$^{1/2}$ (R^2 = 0.77) for magnesium, and 0.35 mg/L/day$^{1/2}$ (R^2 = 0.22) for silicon. Iron was near 0 mg/L throughout the pH 4 and pH 5 50°C experiments. The calcium concentrations for the limestone-cement experiments were too high to measure at pH 5 and were steady throughout the experiments for pH6 and 7. Iron, magnesium and silicon concentrations were steady throughout all of the 50°C limestone-cement experiments.

X-ray maps for the 6-month room temperature pH 3 sandstone-cement sample (Figure 7) made at the 0-degree position show uniform distributions for iron and silicon throughout the cement. The x-ray map for calcium shows a depletion of calcium between the cement-rock interface and about 500 to 800 μm into the sample. Evident in the depleted zone, approximately 300 μm into the sample, are several large calcium-rich "grains" that are not evident in the maps for iron and silicon and are different in size from the other calcium-rich areas shown in the map.

4 Discussion

The linear increase of the depth of penetration of the visible reaction zone in the sandstone-cement experiments versus the Boltzmann variable over the first 6 months indicates that the rate of attack is diffusion-controlled. Islam, Catalan, and Yanful [5] also found a diffusion dependence for the rate of reaction in cement being attacked by acid. The change in slope of the depth of penetration versus the Boltzmann variable between 6 and 12 months may indicate that the dominant reaction controlling the depth of penetration has changed. If the change in slope were an indication that the reaction had stopped, then a similar plateau in the concentration of

calcium should be visible in concentration data (Figure 6) around the same time, and it is not.

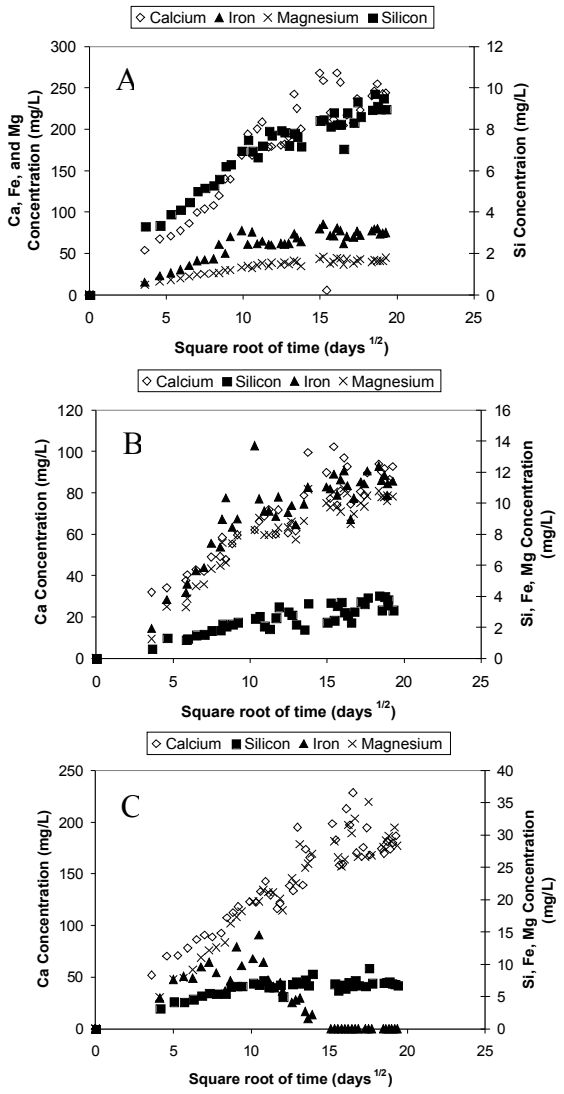

Figure 6 Concentrations of calcium, iron, magnesium, and silicon versus the square root of time for pH 3 (A), pH 4 (B), and pH 5 (C) sandstone-cement experiments.

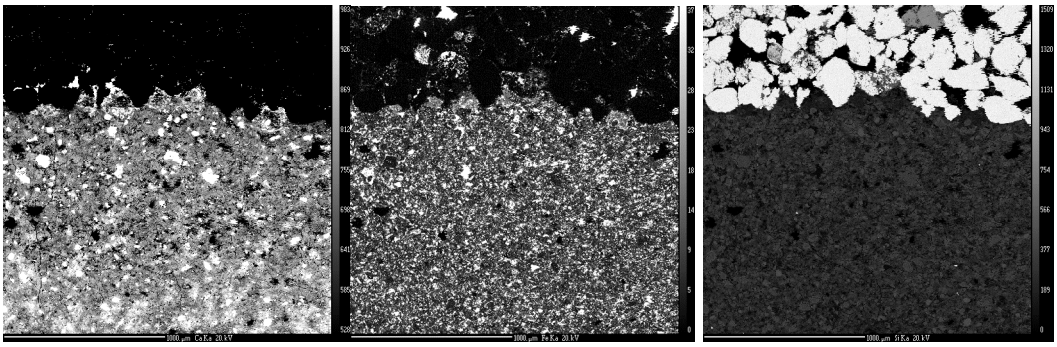

Figure 7 X-ray maps for the 6-month, pH 3 sandstone-cement sample at the 0-degree position for calcium (left), iron (center), and silicon (right). *Note:* The scale bar in the x-ray maps is 1000 μm, and the sandstone is at the top of the maps.

The x-ray maps of the 6-month room temperature sandstone-cement sample (Figure 7) show several calcium-rich grains of material about 300 μm into the cement in the sample; this is approximately the same depth at which the visible reaction in the room temperature samples slowed. The "grains" in the calcium map do not have corresponding locations in the iron or silicon maps, and so they are probably not unreacted cement grains or cement reaction products. This implies that they are either $Ca(OH)_2$ or $CaCO_3$. $Ca(OH)_2$ should be one of the first cement phases to react and be removed from the cement [6], and in previous work [7] we have shown using x-ray diffraction that the orange layer is depleted of $Ca(OH)_2$; thus it seems unlikely that large crystals of $Ca(OH)_2$ would be present after 6 months of reaction. This leaves $CaCO_3$, which is a reaction product of the carbonation of $Ca(OH)_2$ or C-S-H. Equations 1 and 2 show the cement carbonation reactions that may lead to the precipitation of $CaCO_3$. If $CaCO_3$ were to precipitate and block some of the larger pores in the reaction zone, then the removal of cement material might be slowed down, causing a change in the rate at which the visible reaction proceeds into the cement.

$$Ca(OH)_2(s) + H^+ + HCO_3^- \rightarrow CaCO_3(s) + 2H_2O \quad (1)$$

$$C\text{-}S\text{-}H(s) + H^+ + HCO_3^- \rightarrow CaCO_3(s) + S\text{-}H(s) \quad (2)$$

The slowing of the increase in concentration of calcium, iron, magnesium, and silicon during the experiment (Figure 6) is, at least, partially due to the removal of samples for measurements without replacement.

The reaction at the thin side of the sandstone-cement samples was the fastest and deepest, with around 250-μm penetration by 3 months at the 0-degree position for the room temperature samples and 430 μm for the 50°C pH 3 sample. The reaction zone on the side with thick stone was much slower, with no measurable depth at the 180-degree position within the first 3 months. Also during the first 3 months, there is little change in the permeability measured in the sandstone. Therefore it seems plausible that the change in the permeability of the room temperature sandstone-cement samples over time is due to damage in the cement on the side of the sample with thin stone. In fact, the increase in permeability of the room temperature sandstone-cement samples corresponds to flow through a cylindrical hole 400 μm in diameter. Thus, it seems that enough damage occurred between 0 and 1 month for the room temperature pH 3 sample and 0 and 3 months for the room temperature pH 5 sample to control the permeability of the sample for the duration of the experiment. This indicates that the damage on the thin side of the stone after 1 or 3 months (for pH 3 and 5) is minimal, and so is the damage on the thick side of the stone; otherwise further increases in permeability would be expected.

The permeability of both the room temperature and 50°C sandstone-cement samples increased about an order of magnitude during the experiments. It is important to note that the increase in the permeability of the 50°C sandstone-cement samples is also seen in the 50°C sandstone samples. This indicates that the increase at 50°C is due to degradation of the stone and not of the cement. Furthermore, because the degradation of the cement in the 50°C experiments took place in the pore structure of the stone and because the volume of the stone filled with cement was small compared with the total volume of the pores, one would expect the degradation of the cement to have little effect on the permeability of the sample. There was no increase in permeability of the room temperature sandstone samples, so the increase in permeability of the room temperature sandstone-cement samples is due to the degradation of the cement at the cement-rock interface.

The variability in the permeability measurements in the limestone samples is likely a consequence of the variation in the cracks that formed near the 0-degree position during curing. There is no obvious trend in the limestone-cement sample permeabilities during the experiment.

5 Conclusions

Under the conditions of these experiments, the cement at the cement-rock interface in an abandoned petroleum well may be subject to attack, depending on the composition of the stone that makes up the host formation. Class H well cement embedded in sandstone and exposed to silicon-saturated carbonated brine showed a diffusion-controlled attack during the experiment. The cement also showed visible signs of damage in the cement within a month and an order-of-magnitude increase in the permeability of the sample within the first 3 months of exposure. In contrast, the cement that was embedded in limestone and exposed to calcium-saturated brine showed no visible signs of attack and no increase in permeability over the course of a year.

References

[1] API. API Recommended Practice 10B, American Petroleum Institute, Washington D.C., 1997

[2] R. Bruckdorfer, Carbon dioxide corrosion in oilwell cements, SPE Paper 15176, 1986

[3] D.D. Onan, Effects of supercritical carbon dioxide on well cements, SPE Paper 12593, 1984

[4] T.W. Wolery, R.L. Jarek, Softwar e users manual EQ3/6, version 8, Sandia National Laboratory, 2003.

[5] M. Islam, J. Catalan, E. Yanful, A two-front leach model for cement-stabilized heavy metal waste, Environmental science and technology 38 (2004) 1522-1528

[6] F.J. Ulm, E. Lemarchand, F.H. Heukamp, Elements of chemomechanics of calcium leaching of cement-based materials at different scales, Engineering fracture mechanics 70 (2003) 871-889

[7] A. Duguid, M. Radonjic, R. Bruant, G.W. Scherer, Degradation of well cements exposed to carbonated brine, Proceedings of the 4th annual conference on carbon capture and sequestration, Monitor and Exchange Publications and Forum, Washington D.C., 2005